

NON-LTE CALCULATION OF THE Ni I 676.8 NANOMETER LINE IN A FLARING ATMOSPHERE

M. D. DING,^{1,2} JIONG QIU,² AND HAIMIN WANG²

Received 2002 June 28; accepted 2002 July 24; published 2002 August 1

ABSTRACT

The Ni I 676.8 nm line is used by the *Solar and Heliospheric Observatory* Michelson Doppler Imager to measure the magnetic field and velocity field in the solar atmosphere. We make non-LTE calculations of this line in an atmosphere that is bombarded by an energetic electron beam. This case is associated with the occurrence of solar flares. The electron beam produces nonthermal ionization and excitation of the hydrogen atoms and redistributes the level populations. This results in an enhanced opacity near the Ni I line and an upward shift of its formation height, as well as an increased line source function. We find that the Ni I line may appear in emission in the presence of a fairly strong electron beam and preferentially in a cool atmosphere (i.e., sunspot umbrae/penumbrae). On the other hand, if there is no bombarding electron beam, the profile can hardly turn to emission even though the atmosphere may be heated to higher temperatures through other ways. This result implies that the sign reversal of the longitudinal magnetic field observed in some flare events may not be a true reversal but just an artifact associated with the production of an emission profile.

Subject headings: line: profiles — Sun: activity — Sun: atmosphere — Sun: flares

1. INTRODUCTION

Transient magnetic field changes, or magnetic transients, that are associated with solar flares have been observed by ground-based observatories (Patterson & Zirin 1981; Patterson 1984) and more recently by space instruments (Kosovichev & Zharkova 2001; Qiu & Gary 2002). In some cases, there appears a transient sign reversal of the magnetic fields in sunspots (Patterson 1984; Qiu & Gary 2002). Qiu & Gary (2002) discovered that the transient sign reversal occurs in locations of strong hard X-ray emission and that the time profile of the reversed magnetic flux coincides well with the hard X-ray light curve. Patterson (1984) proposed that the magnetic sign reversal is produced by transient emission of the iron line used by the Big Bear Solar Observatory magnetograph. Qiu & Gary (2002) simulated in detail the influence of the line shape on the measurements and concluded that only an emission profile can lead to the observed magnetic sign reversal.

Recent investigations (e.g., Kosovichev & Zharkova 2001; Wang et al. 2002; Qiu & Gary 2002) mostly employ magnetograms observed by the Michelson Doppler Imager (MDI) instrument on board the *Solar and Heliospheric Observatory* (SOHO), which uses the Ni I 676.8 nm line to measure the velocity field and magnetic field (Scherrer et al. 1995). Formation of this line in the quiet-Sun atmosphere was investigated in detail by Bruls (1993), whose results confirm that the line is a good choice for study of helioseismology. In the quiet atmosphere, the Ni I 676.8 nm line is of photospheric origin and appears in absorption. However, in active regions, where the physical conditions can be quite different from that in the quiet Sun, the shape of the line profile may change to affect quantitatively or even qualitatively the measurement results. It is thus desirable to learn how the line is formed in a flare atmosphere, in particular, in what circumstances the profile turns to emission to produce the sign reversal as reported by Qiu & Gary (2002).

There is, however, no observational report of the line profile

in flares. In this Letter, we study the formation of this line through non-LTE calculations. To this end, we first check what physical processes happen at the sites of magnetic polarity reversal. For the event studied by Qiu & Gary (2002), there is a close relationship between the time profile of the reversed magnetic flux and the hard X-ray light curve, implying that the polarity reversal is associated with a precipitating non-thermal electron beam. It has been known that an electron beam helps enhance hydrogen line emission significantly (e.g., Fang, Hénoux, & Gan 1993; Kasparová & Heinzel 2002). In this work, we show that the electron beam is also a key factor in producing an emission profile of the Ni I 676.8 nm line.

2. CALCULATIONS AND RESULTS

2.1. The Atomic Model of Ni I

We use the confection model atom of Ni I proposed by Bruls (1993), which is a simplified version of the comprehensive model. The confection model comprises 10 bound levels, the first four of which are metastable. As shown by Bruls (1993), the confection model yields an Ni I 676.8 nm line profile that is very close to that by the comprehensive model (with a deviation of $\leq 1\%$). As our interest is concentrated on how the line profile changes in different atmospheres, this atomic model should be accurate enough for our study.

2.2. The Atmospheric Models

Flares can occur in different circumstances and, during the development of flares, the atmosphere can be heated to different extents. Therefore, we consider three different model atmospheres, which are, from cool to hot, the penumbral model of Ding & Fang (1989), the quiet-Sun model VAL3C (Vernazza, Avrett, & Loeser 1981), and the flare model F1 (Machado et al. 1980). They represent different preflare conditions or different phases for a specific flare. For each model atmosphere, we assume there is a beam of energetic electrons precipitating from the corona.

We first make non-LTE calculations for the hydrogen atom taking into account the nonthermal collisional (excitation and ionization) rates in the statistical equilibrium equation. The program used here is a revised version of that used by Fang

¹ Department of Astronomy, Nanjing University, 22 Hankou Lu, Nanjing, Jiangsu 210093, China.

² Center for Solar Research, Physics Department, New Jersey Institute of Technology, 323 Martin Luther King Boulevard, Newark, NJ 07102-1982.

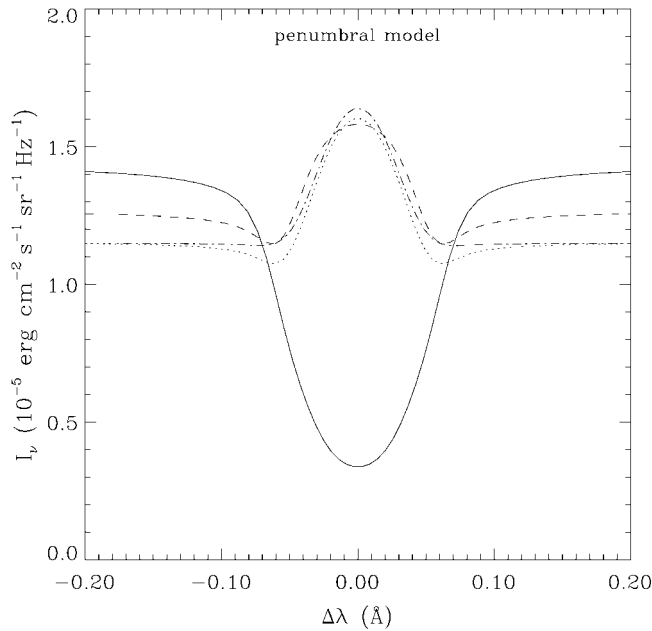


FIG. 1.—Line profiles of Ni I 676.8 nm at disk center calculated from the penumbral model atmosphere of Ding & Fang (1989), bombarded by an electron beam of energy fluxes $\mathcal{F}_1 = 0$ (solid curve), 10^9 (dashed curve), 10^{10} (dotted curve), and 10^{11} (dash-dotted curve) $\text{ergs cm}^{-2} \text{s}^{-1}$.

et al. (1993). The atomic model of hydrogen consists of five bound levels plus continuum. Having obtained the level populations of hydrogen and the electron density, we then perform the non-LTE calculations for the Ni I atom using the code MULTI (version 2.2) by Carlsson (1986).

Note that statistical equilibrium is a reasonable assumption if the timescale of beam injection is long enough (several seconds or longer). In a case of short-period (subsecond) beam injection, one needs to solve the time-dependent rate equations instead (e.g., Ding et al. 2001).

2.3. The Ni I Line Profile

In Figures 1–3, we plot the Ni I 676.8 nm line profiles at disk center calculated from the three model atmospheres. For each model, we consider four different cases of electron beams, with an energy flux $\mathcal{F}_1 = 0, 10^9, 10^{10}$, and 10^{11} $\text{ergs cm}^{-2} \text{s}^{-1}$, respectively. The first one corresponds to a case of no beam (i.e., in situations before flare eruption or when the atmosphere is heated through other ways than by the particle beam) and the latter three to cases of weak, moderate, and strong beams, respectively. A definite value of beam flux in a real event can be derived from the hard X-ray spectra if available (e.g., Fang et al. 1998). As usual, we assume a power-law distribution for each beam with a power index $\delta = 4$ and a low-energy cutoff $E_1 = 20$ keV. Note that these two parameters may vary from case to case, but changing them does not alter the qualitative results below.

As shown in Figures 1–3, in the case of no electron beam, the Ni I line remains in absorption from a cool to a hot atmosphere. The only change is an increase of the absolute intensity and the line width. We have checked more models and found that within the range of available flare models, the Ni I line cannot turn to emission although it can become shallower and broader. The situation becomes quite different if we consider the role of an electron beam. In particular, in a cool atmosphere, such as the sunspot penumbral atmosphere, the line changes from absorption to emission as soon as the beam sets in. In comparison,

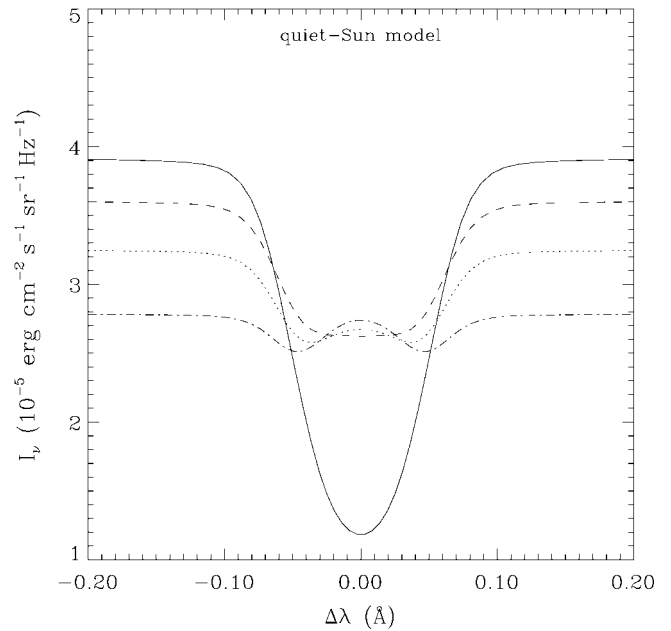


FIG. 2.—Same as Fig. 1, but for the quiet-Sun model atmosphere VAL3C (Vernazza et al. 1981).

in a quiet-Sun or flare atmosphere, it is relatively hard, though still possible, to produce an emission profile. In the latter case, a relatively strong electron beam (say, $\mathcal{F}_1 \geq 10^{10}$ $\text{ergs cm}^{-2} \text{s}^{-1}$) is required, and the emission amplitude seems rather small.

2.4. The Opacity

The Ni I 676.8 nm line lies in the visible (Paschen) continuum. In the lower chromosphere and below, the continuum opacity is mainly contributed by the hydrogen photoionization (H_{bf}) and the absorption of negative hydrogen ions (H_{br}^- and H_{fr}^-). Usually, the line opacity is much greater than the background continuum opacity (Fig. 4a). However, in the case of electron beam heating, the beam produces nonthermal excita-

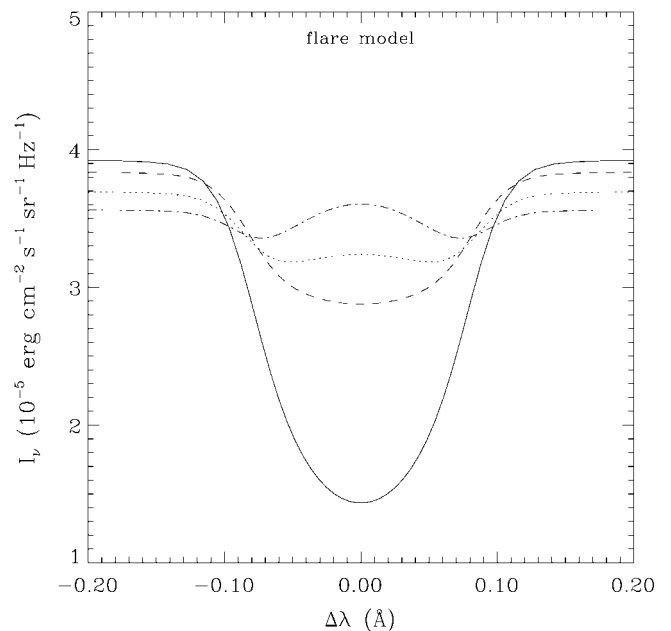


FIG. 3.—Same as Fig. 1, but for the flare model atmosphere F1 (Machado et al. 1980).

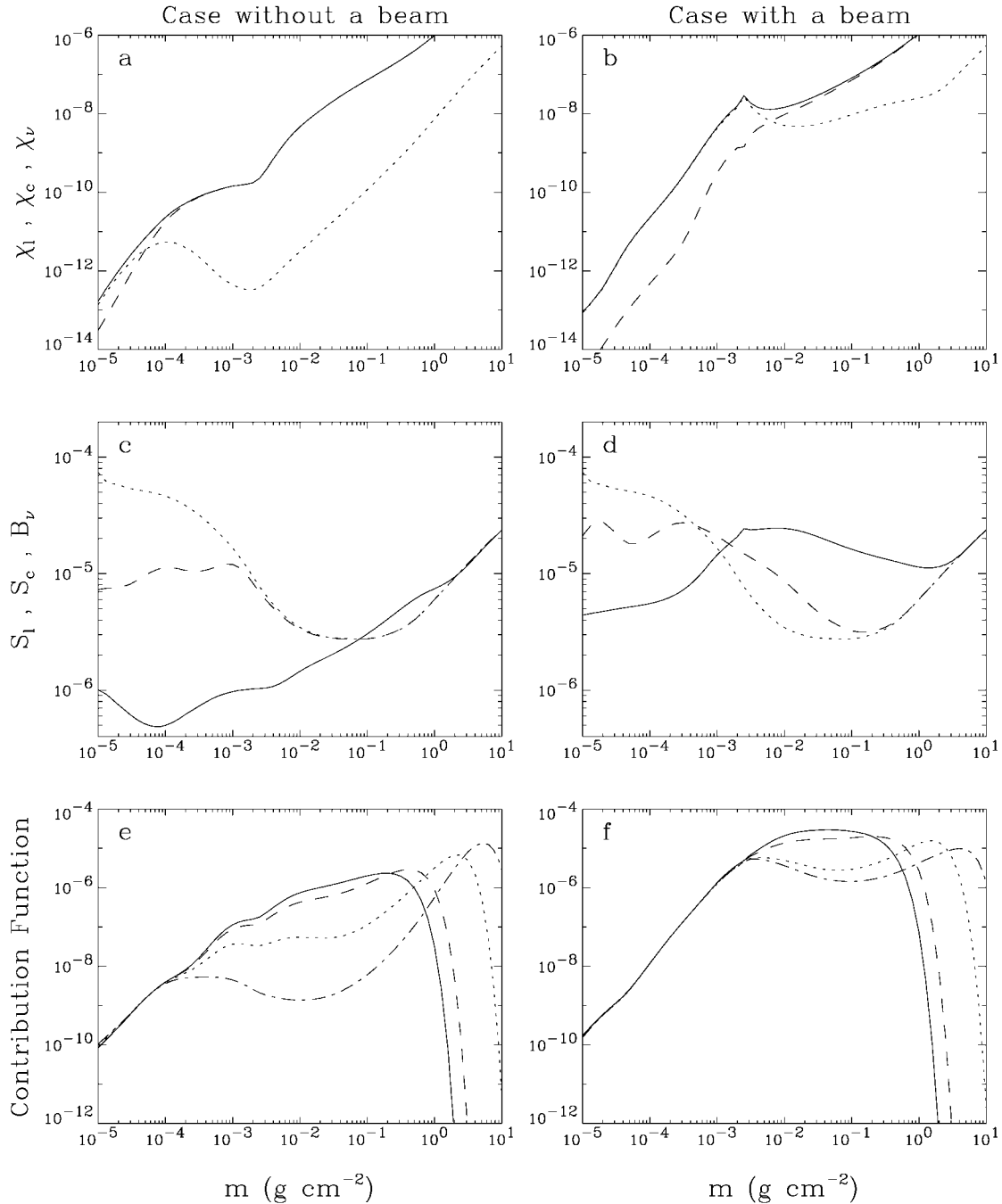


FIG. 4.—Opacity (*top row*), source function (*middle row*), and contribution function (*bottom row*) computed from the penumbral model atmosphere (Ding & Fang 1989) for two different cases without any electron beam (*left column*) and with an electron beam of $T_e = 10^{10}$ ergs $\text{cm}^{-2} \text{s}^{-1}$ (*right column*). In (*a*) and (*b*), solid curves are for the total opacity, dashed curves the line opacity (at line center), and dotted curves the background opacity. In (*c*) and (*d*), solid curves are for the line source function and dashed curves are for the continuum source function, while dotted curves refer to the Planck function. In (*e*) and (*f*), from left to right, the four curves refer to contribution function to the line intensity at $\Delta\lambda = 0.000, 0.025, 0.054,$ and 0.141 \AA , respectively, on a $\log \tau$ scale. All the quantities are in cgs units.

tion and ionization effects. As a consequence, more hydrogen atoms are excited to higher levels or ionized, and the electron density is increased. Therefore, the continuum opacity undergoes a drastic change; it is enhanced by orders of magnitude in chromospheric layers (Fig. 4*b*). On the contrary, the change of the line opacity of Ni I 676.8 nm is much less obvious. It is seen that in the lower chromosphere, the continuum opacity even grows to exceed the line opacity. The direct consequence of an enhanced total opacity is to shift the formation height of the line upward. This can be seen from the change of the contribution function to the line intensity from thermal to non-

thermal cases (Figs. 4*e* and 4*f*). One notices that in the non-thermal case, the chromospheric contribution to the line intensity, in particular to that at the line center, increases significantly.

2.5. The Source Function

The Ni I 676.8 nm line corresponds to a transition between levels z^3P^o and a^1S . Level a^1S is metastable and is populated through collisional excitation from lower levels and deexcitation from higher levels. For level z^3P^o , however, photoex-

citation from lower levels is relatively important among the various transitions to this level. Within the line, the radiative rates are much greater than the collisional rates. Therefore, the line source function depends more on the radiation field; it usually deviates from the Planck function above the photosphere.

As shown in Figure 4c, in the case of no electron beam heating, the line source function decreases almost monotonically with height. When an electron beam sets in, radiation in the hydrogen Paschen continuum is enhanced, in particular in chromospheric layers where the electron beam deposits most of its energy. This forms a locally elevated (angle-averaged) continuum background near the Ni I line, as well as an enhanced continuum source function, in and around these layers. The line source function even increases by as much as an order of magnitude; it forms a local maximum in the lower chromosphere (Fig. 4d).

2.6. Discussion

Now it is clear that the increased line source function in the chromosphere and the enhanced background opacity are the cause of an emission profile of the Ni I 676.8 nm line. The nonthermal electron beam plays the key role in reversing the profile from absorption to emission. As noted above, without the nonthermal effect, a model atmosphere, even with a higher temperature to fit some flare spectra, such as H and Ca II lines (e.g., Machado et al. 1980; Avrett, Machado, & Kurucz 1986; Mauas, Machado, & Avrett 1990; Ding et al. 1994), can hardly produce an emission profile of the Ni I 676.8 nm line.

On the other hand, an emission profile of the Ni I 676.8 nm line appears preferentially in a cooler atmosphere. This fact can be understood since the role of a nonthermal electron beam is more effective in a cool atmosphere than in a hot atmosphere. If we select an umbral model instead of the penumbral model to represent the cool atmosphere, the conclusion remains the same. In this case, it is even easier to turn the Ni I line into emission. Besides, we find that the intensity in the far wings decreases when an electron beam sets in (while the atmosphere remains unchanged otherwise), contrary to the case of the line core. The line wings originate mostly from the photosphere. When an electron beam exists, the chromospheric contribution to the line wing intensity increases; however, the increased opacity in the chromosphere reduces the photospheric contribution (Fig. 4f), which leads finally to a decreased line wing

intensity. Such a phenomenon is also used to explain the continuum dimming at the very beginning of flares (Hénoux et al. 1990; Ding & Fang 2000).

3. CONCLUSIONS

Through non-LTE calculations, we have investigated the formation of the Ni I 676.8 nm line in an atmosphere bombarded by a nonthermal electron beam. We find that the electron beam plays the key role in changing the shape of the line profile. First, the beam produces nonthermal collisional excitation and ionization of the hydrogen atoms; this effect results in an enhanced electron density and an enhanced radiation field at the continuum background in the chromosphere. Consequently, the Ni I line source function is increased; the background opacity near the line is increased as well to shift the formation height of the line upward. Therefore, the line may change from absorption to emission if the beam is fairly strong. Such a case appears preferentially in a cooler atmosphere (e.g., sunspot umbrae/penumbrae). On the contrary, if there is no electron beam, the line can hardly turn to emission even though the atmosphere can be heated to higher temperatures through other ways. We note that the two factors, a cooler atmosphere and a precipitating electron beam, which favor the production of an emission profile of Ni I 676.8 nm, are nicely compatible with observations (Qiu & Gary 2002).

The above results provide a theoretical support to the argument that the sign reversal of magnetic fields in solar active regions observed by *SOHO/MDI* is due to the change of a profile from absorption to emission (Qiu & Gary 2002). It implies that, at least in some cases, the observed sign reversal is only an artifact but not a true reversal. In future studies, caution must be taken in dealing with the observed sign reversal of magnetic (velocity) fields observed by MDI, especially in locations that are relatively cool and are possibly heated by electron beams.

We thank J. Bruls for providing the atomic model of Ni I and for valuable comments on the manuscript. This work was supported by NSF under grants AST 99-87366, ATM 00-76602, and ATM 00-86999, by NASA under grants NAG5-9501, NAG5-9682, NAG5-10212, and NAG5-10910, and by ONR under grant N00014-97-1-1037. M. D. D. was also supported by TRAPOYT, NKBRSE, under grant G20000784, and NSFC under grant 10025315.

REFERENCES

- Avrett, E. H., Machado, M. E., & Kurucz, R. L. 1986, in *The Lower Atmosphere of Solar Flares*, ed. D. F. Neidig (Sunspot: NSO), 216
- Bruls, J. H. M. J. 1993, *A&A*, 269, 509
- Carlsson, M. 1986, *A Computer Program for Solving Multi-Level Non-LTE Radiative Transfer Problems in Moving or Static Atmospheres* (Uppsala Astron. Obs. Rep. 33; Uppsala: Uppsala Univ.)
- Ding, M. D., & Fang, C. 1989, *A&A*, 225, 204
- . 2000, *MNRAS*, 317, 867
- Ding, M. D., Fang, C., Gan, W. Q., & Okamoto, T. 1994, *ApJ*, 429, 890
- Ding, M. D., Qiu, J., Wang, H., & Goode, P. R. 2001, *ApJ*, 552, 340
- Fang, C., Hénoux, J.-C., & Gan, W. Q. 1993, *A&A*, 274, 917
- Fang, C., Tang, Y. H., Hénoux, J.-C., Huang, Y. R., Ding, M. D., & Sakurai, T. 1998, *Sol. Phys.*, 182, 163
- Hénoux, J.-C., Aboudarham, J., Brown, J. C., van den Oord, G. H. J., van Driel-Gesztelyi, L., & Gerlei, O. 1990, *A&A*, 233, 577
- Kasparová, J., & Heinzel, P. 2002, *A&A*, 382, 688
- Kosovichev, A. G., & Zharkova, V. V. 2001, *ApJ*, 550, L105
- Machado, M. E., Avrett, E. H., Vernazza, J. E., & Noyes, R. W. 1980, *ApJ*, 242, 336
- Mauas, P. J., Machado, M. E., & Avrett, E. H. 1990, *ApJ*, 360, 715
- Patterson, A. 1984, *ApJ*, 280, 884
- Patterson, A., & Zirin, H. 1981, *ApJ*, 243, L99
- Qiu, J., & Gary, D. E. 2002, *ApJ*, submitted
- Scherrer, P. H., et al. 1995, *Sol. Phys.*, 162, 129
- Vernazza, J. E., Avrett, E. H., & Loeser, R. 1981, *ApJS*, 45, 635
- Wang, H., Spirock, T. J., Qiu, J., Ji, H., Yurchyshyn, V., Moon, Y.-J., Denker, C., & Goode, P. R. 2002, *ApJ*, in press